

A THEORETICAL APPROACH FOR PREDICTING NUMBER OF TURNS AND CYCLONE PRESSURE DROP

L. Wang, C. B. Parnell, B. W. Shaw, R. E. Lacey

ABSTRACT. A new theoretical method for computing travel distance, number of turns, and cyclone pressure drop has been developed and is presented in this article. The flow pattern and cyclone dimensions determine the travel distance in a cyclone. The effective number of turns was calculated based on the travel distance. Cyclone pressure drop is composed of five pressure loss components. The frictional pressure loss is the primary pressure loss in a cyclone. This new theoretical analysis of cyclone pressure drop for 1D2D, 2D2D, and 1D3D cyclones was tested against measured data at different inlet velocities and gave excellent agreement. The results show that cyclone pressure drop varies with the inlet velocity, but not with cyclone diameter.

Keywords. Cyclone, Number of turns, Pressure drop, 1D2D cyclone, 2D2D cyclone, 1D3D cyclone.

Cyclone separators provide a method of removing particulate matter from air streams at low cost and low maintenance. In general, a cyclone consists of an upper cylindrical part referred to as the barrel and a lower conical part referred to as the cone (fig. 1). The air stream enters tangentially at the top of the barrel and travels downward into the cone, forming an outer vortex. The increasing air velocity in the outer vortex results in a centrifugal force on the particles, separating them from the air stream. When the air reaches the bottom of the cone, an inner vortex is created, reversing direction and exiting out the top as clean air while the particulates fall into the dust collection chamber attached to the bottom of the cyclone.

In the agricultural processing industry, 2D2D (Shepherd and Lapple, 1939) and 1D3D (Parnell and Davis, 1979) cyclone designs are the most commonly used abatement devices for particulate matter control. The D in the 2D2D designation refers to the barrel diameter of the cyclone. The numbers preceding each D relate to the length of the barrel and cone sections, respectively. A 2D2D cyclone has barrel and cone lengths two times the barrel diameter, whereas a 1D3D cyclone has a barrel length equal to the barrel diameter and a cone length of three times the barrel diameter. Parnell and Davis (1979) first developed a 1D3D cyclone for cotton gins in an attempt to provide a more efficient fine dust collector. This cyclone design is referred to as the traditional

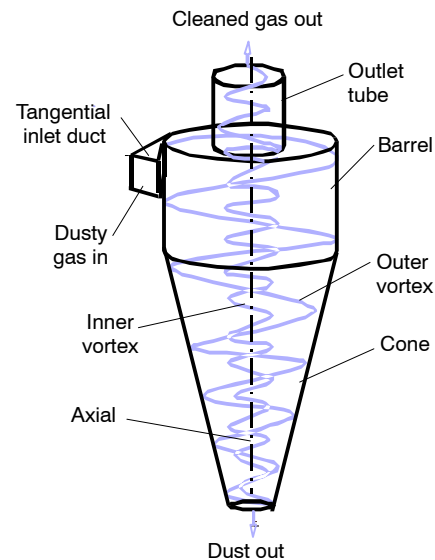


Figure 1. Schematic flow diagram of a cyclone separator.

1D3D cyclone (fig. 2). Holt and Baker (1999) and Funk et al. (1999) conducted further experimental research on this cyclone design and reported a significant improvement in efficiency by modifying the traditional 1D3D design to employ a 2D2D inlet (fig. 2). This modified 1D3D cyclone design is referred to as 1D3D in this article.

The configuration of a 2D2D cyclone is illustrated in figure 3. Previous research (Wang, 2000) indicated that, compared to other cyclone designs, 1D3D and 2D2D are the most efficient cyclone collectors for fine dust (particle diameters less than 100 μm). Mihalski et al (1993) reported “cycling lint” near the trash exit for the 1D3D and 2D2D cyclone designs when the PM in the inlet air stream contained lint fiber. Mihalski reported a significant increase in the exit PM concentration for these high efficiency cyclone designs and attributed this to small balls of lint fiber “cycling” near the trash exit causing the fine PM that would normally be collected to be diverted to the clean air exit stream. Simpson

Submitted for review in April 2004 as manuscript number SE 5302; approved for publication by the Structures & Environment Division of ASABE in March 2006. Presented at the 2001 ASAE Annual Meeting as Paper No. 014009.

The authors are **Lingjuan Wang, ASABE Member Engineer**, Assistant Professor, Department of Biological and Agricultural Engineering, North Carolina State University, Raleigh, North Carolina; and **Calvin B. Parnell, ASABE Fellow Engineer**, Regents Professor, **Bryan W. Shaw, ASABE Member Engineer**, Associate Professor, and **Ronald E. Lacey, ASABE Member Engineer**, Professor, Department of Biological and Agricultural Engineering, Texas A&M University, College Station, Texas. **Corresponding author:** Lingjuan Wang, Department of Biological and Agricultural Engineering, North Carolina State University, Raleigh, NC 27695-7625; phone: 919-515-6762; fax: 919-515-7760; e-mail: Lwang5@ncsu.edu.

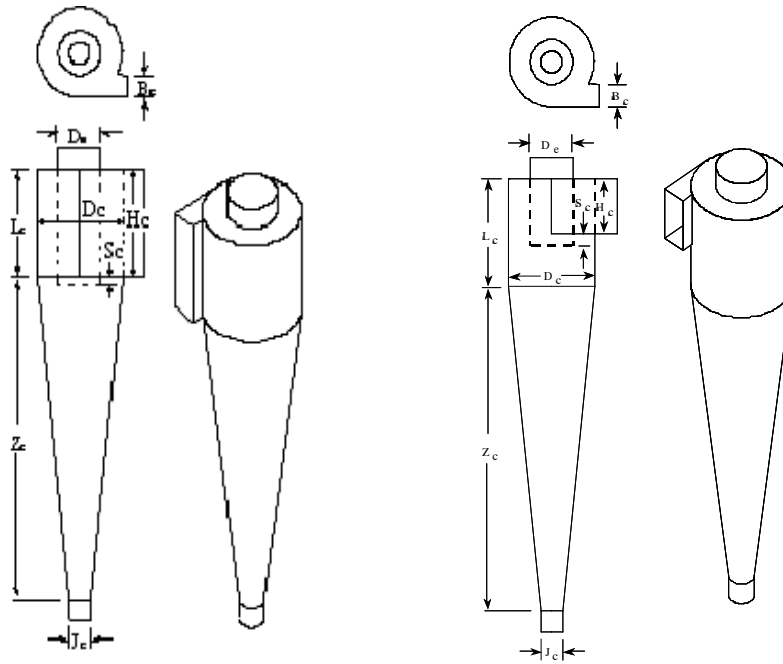


Figure 2. Traditional 1D3D cyclone (left) and 1D3D cyclone with 2D2D inlet (right).

Traditional 1D3D cyclone: $B_c = D_c/8$ $J_c = D_c/4$ $D_e = D_c/2$ $S_c = D_c/8$ $H_c = 1 \times D_c$ $L_c = 1 \times D_c$ $Z_c = 3 \times D_c$

1D3D cyclone w/2D2D inlet: $B_c = D_c/4$ $J_c = D_c/4$ $D_e = D_c/2$ $S_c = D_c/8$ $H_c = D_c/2$ $L_c = 1 \times D_c$ $Z_c = 3 \times D_c$

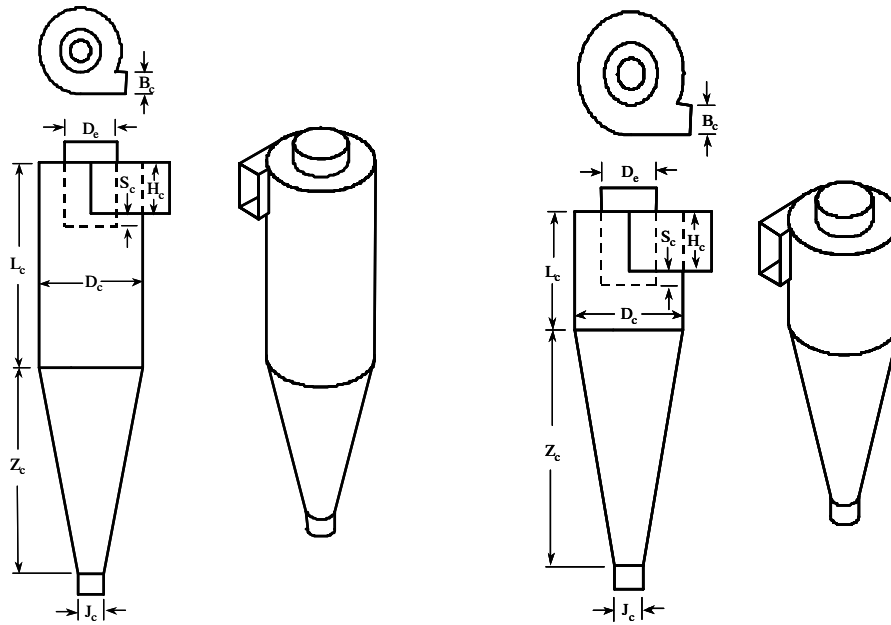


Figure 3. 2D2D cyclone (left) and 1D2D cyclone (right).

2D2D cyclone: $B_c = D_c/4$ $J_c = D_c/4$ $D_e = D_c/2$ $S_c = D_c/8$ $H_c = D_c/2$ $L_c = 2 \times D_c$ $Z_c = 2 \times D_c$

1D2D cyclone: $B_c = D_c/4$ $J_c = D_c/2$ $D_e = D_c/1.6$ $S_c = 5D_c/8$ $H_c = D_c/2$ $L_c = 1 \times D_c$ $Z_c = 2 \times D_c$

and Parnell (1995) introduced a new low-pressure cyclone, called the 1D2D cyclone, for the cotton ginning industry to solve the cycling-lint problem. The 1D2D cyclone is a better

design for high-lint content trash compared with 1D3D and 2D2D cyclones (Wang et al., 1999). The configuration of 1D2D cyclone is illustrated in figure 3.

THE CLASSICAL CYCLONE DESIGN

METHOD

Several methods or procedures are used by engineers to design cyclones. The design procedures outlined in *Air Pollution Engineering Manual* (Davis, 2000) and *Air Pollution Control: A Design Approach* (Copper and Alley, 2002) are perceived by some engineers as a standard method. This design process, referred to as classical cyclone design (CCD), requires knowledge of the number of turns, the cutpoint, and the fractional collection efficiency to determine a cyclone's overall collection efficiency. The CCD also includes a model for cyclone pressure drop determination.

The number of effective turns in a cyclone is the number of revolutions that the gas completes while passing through the cyclone. The model for the number of turns included in CCD was developed by Lapple (1951) as:

$$N_e = \frac{1}{H_c} \left[L_c + \frac{Z_c}{2} \right] \quad (1)$$

where

N_e = number of effective turns

H_c = height of inlet duct

L_c = length of barrel body

Z_c = vertical length of cone body.

Mihalski and Kaspar (1992) conducted experiments to determine the number of turns, cutpoints, and collection efficiency. The results from their tests suggest that the measured numbers of turns for 1D3D and 2D2D cyclones are 6.00 and 5.25, respectively, which do not agree with Lapple model predictions (eq. 1). Further research on determination of the number of turns is needed.

In the evaluation of a cyclone design, pressure drop is a primary consideration. Because it is directly proportional to the energy requirement, knowledge of pressure drop through a cyclone is essential in designing a fan system. Shepherd and Lapple (1939) reported that a cyclone's pressure drop was composed of the following components:

- Loss due to expansion of gas when it enters the cyclone chamber.
- Loss as kinetic energy of rotation in the cyclone chamber.
- Loss due to wall friction in the cyclone chamber.
- Any additional friction losses in the exit duct, resulting from the swirling flow above and beyond those incurred by straight flow.
- Any regain of the rotational kinetic energy as pressure energy.

Based on their theoretical analyses, Shepherd and Lapple (1939) developed two empirical models for cyclone pressure drop estimation. The Shepherd and Lapple approach has been considered the simplest to use, and it is included in CCD. These two models are shown in equations 2 and 3:

$$H_v = K \frac{H_c B_c}{D_e^2} \quad (2)$$

where

H_v = pressure drop, expressed in number of inlet velocity heads

K = constant that depends on cyclone configurations and operating conditions ($K = 12$ to 18 for a standard tangential-entry cyclone)

H_c = height of inlet duct

B_c = width of inlet duct.

$$\Delta P = \frac{1}{2} \rho_g V_i^2 H_v \quad (3)$$

where

ΔP = pressure drop (Pa)

ρ_g = gas density (kg/m^3)

V_i = inlet gas velocity (m/s).

OTHER MODELS FOR NUMBER OF TURNS AND PRESSURE DROP PREDICTIONS

Many other models have been developed since the work of Lapple (1951) and Shepherd and Lapple (1939) to determine the number of turns and pressure drop in a cyclone. Table 1 lists several models described in the *Handbook of Powder Science and Technology* (Fayed and Otten, 1997) for predicting cyclone collection characteristics, from which the number of turns can be backwards derived, and table 2 summarizes several other models included in the handbook for cyclone pressure drop prediction. Leith and Mehta (1973) conducted research to compare experimental values of pressure drop with calculated values for each of the pressure drop equations using experimental data drawn from the literature (Shepherd and Lapple, 1940; Stern et al., 1955; Stairmand, 1949, 1951). They concluded that the pressure drop calculation methods proposed by Barth (1956), Stair-

Table 1. Equations for predicting collection characteristics, from which the number of turns can be backwards derived for given d_{100} and d_{50} .

Collection Characteristics	Source	Solutions for $N^{[a]}$
$d_{100}^{[b]} = \left[\frac{9\mu b}{2\pi\rho_p V_i N} \left(1 - \frac{b}{D} \right) \right]^{-\frac{1}{2}}$	Rosin et al. (1932)	1D2D: $N = 0.51$ 2D2D: $N = 0.69$ 1D3D: $N = 0.73$
$d_{100} = \left(\frac{9\mu D_e}{2\pi\rho_p V_i N} \right)^{\frac{1}{2}}$	Shepherd and Lapple (1940)	1D2D: $N = 0.84$ 2D2D: $N = 0.92$ 1D3D: $N = 0.97$
$d_{50}^{[c]} = \left(\frac{9\mu b}{2\pi\rho_p V_i N} \right)^{\frac{1}{2}}$	Lapple (1951)	1D2D: $N = 1.92$ 2D2D: $N = 1.61$ 1D3D: $N = 1.62$

List of symbols:

b = gas entry width = $D/4$

d_{100} = critical particle diameter, theoretically collected with 100% efficiency

d_{50} = critical particle diameter, theoretically collected with 50% efficiency

D = cyclone cylinder diameter

D_e = gas outlet diameter = $D/1.6$ (1D2D) or $D/2$ (2D2D and 1D3D)

N = number of turns

V_i = gas inlet velocity

μ = gas viscosity

ρ_p = particle density.

[a] 1D2D: $V_i = 12.19$ m/s; 2D2D: $V_i = 15.24$ m/s; 1D3D: $V_i = 16.26$ m/s; $D = 0.2$ m; $\rho_p = 2.7$ g/cm³; and $\mu = 1.81 \times 10^{-5}$ N·s/m².

[b] 1D2D: $d_{100} = 10.75$ μm at $d_{50} = 4.5$ μm and $\text{slop} = 1.30$.
2D2D: $d_{100} = 8.25$ μm at $d_{50} = 4.40$ μm and $\text{slop} = 1.20$.
1D3D: $d_{100} = 7.75$ μm at $d_{50} = 4.25$ μm and $\text{slop} = 1.20$ (Wang et al., 2002).

[c] 1D2D: $d_{50} = 4.5$ μm ; 2D2D: $d_{50} = 4.40$ μm ; and 1D3D: $d_{50} = 4.25$ μm (Wang et al., 2002).

mand (1949, 1951), and Shepherd and Lapple (1939, 1940) appeared superior to the methods proposed by Alexander (1949) and First (1950). The Shepherd and Lapple approach was the simplest to use of all the methods considered.

However, the equations are either empirical models or involve variables and dimensionless parameters not easily evaluated in practical applications. It is known (Doerschlag and Miczek, 1977) that cyclone pressure drop is dependent on the cyclone design and on operating parameters such as inlet velocity. The empirical models cannot be used for all cyclone designs as new cyclone technology and new cyclone designs are developed. Further theoretical research is needed

to scientifically evaluate cyclone performance, including predicting cyclone pressure drop.

FLOW PATTERN IN A CYCLONE

A theoretical study of cyclone performance requires knowledge of the characteristics of the internal flow. This knowledge of the flow pattern in a cyclone fluid field is the basis for theoretical considerations for the prediction of the number of effective turns, pressure drop, and dust collection efficiency. Many investigations have been made to determine the flow pattern (velocity profile) in a cyclone rotational

Table 2. Equations for predicting pressure loss at number of inlet velocity heads (H_v).

Pressure Loss Equations	Source	Solutions for H_v
$H_v = \frac{ab}{D_e^2} \left\{ 24 \div \left[\frac{h(H-h)}{D^2} \right]^{\frac{1}{3}} \right\}$	First (1950)	1D2D: $H_v = 6.10$ 2D2D: $H_v = 7.56$ 1D3D: $H_v = 8.32$
$H_v = 4.62 \frac{ab}{DD_e} \left\{ \left[\left(\frac{D}{D_e} \right)^{2n} - 1 \right] \left(\frac{1-n}{n} \right) + f \left(\frac{D}{D_e} \right)^{2n} \right\}$ $n = 0.67 D_m^{0.14} \text{ at } 283 \text{ K } \frac{1-n_1}{1-n_2} = \left(\frac{T_1}{T_2} \right)$ $f = 0.8 \left[\frac{1}{n(1-n)} \left(\frac{4-2^{2n}}{3} \right) - \left(\frac{1-n}{n} \right) \right] + 0.2 \left[(2^{2n}-1) \left(\frac{1-n}{n} \right) + 1.5(2^{2n}) \right]$	Alexander (1949)	1D2D: $H_v = 3.77$ 2D2D: $H_v = 6.21$ 1D3D: $H_v = 6.21$ $D_m = 0.2m$ $n_1 = 0.535$ $n_2 = 0.517$
$H_v = 1 + 2\phi^2 \left[\frac{2(D-b)}{D_e} - 1 \right] + 2 \left(\frac{4ab}{\pi D_e^2} \right)^2$ $\phi = \frac{- \left[\frac{D_e}{2(D-b)} \right]^{\frac{1}{2}} + \left[\frac{D_e}{2(D-b)} + \frac{4G^* A}{ab} \right]^{\frac{1}{2}}}{\frac{2G^* A}{ab}}$ $A = \frac{\pi}{4} (D^2 - D_e^2) + \pi D h + \pi D_e S + \frac{\pi}{2} (D+B) \left[(H-h)^2 + \left(\frac{D-B}{2} \right)^2 \right]^{\frac{1}{2}}$	Stairmand (1949)	1D2D: $H_v = 2.04$ 2D2D: $H_v = 3.35$ 1D3D: $H_v = 3.03$
$H_v = \left(\frac{4ab\theta}{\pi D_e^2} \right)^2 \epsilon$ $\epsilon = \frac{D_e}{D} \left\{ \frac{1}{[1 - 2\theta(H-S)(\lambda/D_e)]^2} - 1 \right\} + 4.4\theta^3 + 1$ $\theta = \frac{\pi D_e (D-b)}{4ab\alpha^* + 2(H-S)(D-b)\pi\lambda} \quad \alpha^* = 1 - \frac{1.2b}{D}$	Barth (1956)	1D2D: $H_v = 5.09$ 2D2D: $H_v = 8.51$ 1D3D: $H_v = 8.51$
<p>List of symbols:</p> <ul style="list-style-type: none"> a = gas entry height A = inside surface area of cyclone b = gas entry width B = dust outlet diameter D = cyclone cylinder diameter D_e = gas outlet diameter D_m = cyclone cylinder diameter (m) f = factor G^* = friction factor (0.005) 	<ul style="list-style-type: none"> h = cyclone cylinder height H = cyclone overall height n = vortex exponent S = gas outlet height T = absolute temperature α = factor ϵ = loss factor θ = ratio of maximum tangential gas velocity to gas velocity in gas outlet λ = friction factor (0.02) ϕ = ratio of maximum tangential gas velocity to velocity within gas entry. 	

field. Shepherd and Lapple (1939) reported that the primary flow pattern consisted of an outer spiral moving downward from the cyclone inlet and an inner spiral of smaller radius moving upward into the exit pipe (known as outer vortex and inner vortex). The transfer of fluid from the outer vortex to the inner vortex apparently began below the bottom of the outer vortex and continued down into the cone to a point near the dust outlet at the bottom of the cyclone. They concluded from streamer and pitot tube observations that the radius marking the outer limit of the inner vortex and the inner limit of the outer vortex was roughly equal to the exit duct radius. Ter Linden (1949) measured the details of the flow field in a 36 cm (14 in.) cyclone. He reported that the interface of the inner vortex and outer vortex occurred at a radius somewhat less than that of the exit duct in the cylindrical section of the cyclone and approached the centerline in the conical section. In this research, the interface diameter was assumed to be the cyclone exit tube diameter ($D_o = D_e$).

The velocity profile in a cyclone can be characterized by three velocity components (tangential, axial, and radial). The tangential velocity is the dominant velocity component. It also determines the centrifugal force applied to the air stream and to the particles. Research results of Shepherd and Lapple (1939), Ter Linden (1949), and First (1950) indicated that tangential velocity in the annular section (at the same cross-sectional area) of the cyclone could be determined by:

$$V_t * r^n = C_1 \quad (4)$$

where

- V_t = tangential velocity
- r = air stream rotational radius
- n = flow pattern factor ($n = 0.5$ in outer vortex)
- C_1 = numerical constant.

A NEW THEORETICAL METHOD

One hypothesis in this research is that the air stream travel distance in the outer vortex and the cyclone dimensions determine the number of turns. The travel distance can be calculated mathematically by the velocity and travel time. A cyclone consists of a cylinder upper body (barrel) with a conical lower section (fig. 1). In the barrel, there are two velocity components: tangential velocity (V_t) and axial velocity (V_z). The airflow rate is constant in the barrel, so the tangential velocity and the axial velocity can be considered as constant, too. In the cone, the air stream is squeezed. As a result, air leaks from the outer vortex to the inner vortex through their interface. It is assumed that the air leak (airflow rate) follows a linear model from the top of the cone to the intersection of vortex interface and the cone walls. This assumption yields an effective length for the dust collection (Z_o , fig. 4). There are three velocity components in the cone: tangential velocity (V_t), axial velocity (V_z), and radial velocity (V_r).

TRAVEL DISTANCE AND NUMBER OF TURNS IN THE BARREL (L_1 AND N_1)

There are two velocity components in the barrel: tangential velocity (V_{t1}) and axial velocity (V_{z1}). It is assumed that tangential velocity is equal to the inlet velocity for the tangential inlet design ($V_{t1} = V_{in}$). The axial velocity can be calculated based on the constant airflow rate:

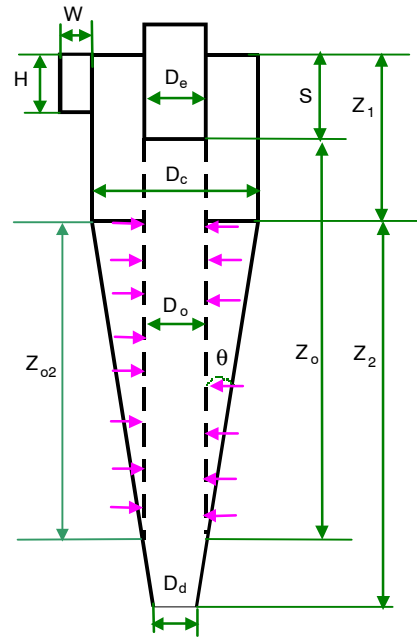


Figure 4. Air stream vortex interface (D_o) and effective length (Z_o) in a cyclone.

$$V_{z1} \left(\frac{\pi * D_c^2}{4} - \frac{\pi * D_e^2}{4} \right) = V_{in} * \frac{D_c^2}{8} \quad (5)$$

where

- V_{z1} = axial velocity in the barrel
- V_{in} = inlet velocity
- D_c = cyclone diameter
- D_e = air exit tube diameter.

Then:

$$V_{z1} = \frac{2V_{in}}{3\pi} \quad (\text{for 1D3D and 2D2D designs})$$

$$V_{z1} = \frac{32V_{in}}{39\pi} \quad (\text{for 1D2D design})$$

The total average velocity and travel distance in the barrel can be obtained using the following equations:

$$V_1 = \sqrt{V_{t1}^2 + V_{z1}^2} \quad (6)$$

$$L_1 = \int_0^{t_1} V_1 * dt = \int_0^{z_1} V_1 * \frac{dz}{V_{z1}} \quad (7)$$

where

- L_1 = travel distance in the barrel
- V_1 = total average velocity in the barrel at time t
- Z_1 = length of the barrel
- dz = axial component of travel distance during the time dt .

Then:

$$L_1 = 1.53 * \pi * Z_1 \quad (\text{for 1D3D and 2D2D designs})$$

$$L_1 = 1.26 * \pi * Z_1 \quad (\text{for 1D2D design})$$

The following equation can be used to approximately estimate the number of turns in the barrel:

$$N_1 = \frac{L_1}{\pi * D_c} \quad (8)$$

where

N_1 = number of turns in the barrel
 L_1 = travel distance in the barrel
 D_c = cyclone diameter.

Then:

$N_1 = 1.53$ (for 1D3D)
 $N_1 = 3.06$ (for 2D2D)
 $N_1 = 1.26$ (for 1D2D)

TRAVEL DISTANCE AND NUMBER OF TURNS IN THE CONE (L_2 AND N_2)

In the cone, the flow pattern becomes more complex. Three velocity components are involved in the total velocity calculation: tangential velocity (V_{t2}), axial velocity (V_{z2}), and radial velocity (V_{r2}). The tangential velocity in the cone can be determined by equation 5. In developing the equations for the velocity components, the following assumptions are made:

- The diameter (D_o) of the interface of the inner vortex and outer vortex is equal to the exit tube diameter (D_e) (fig. 4).
- The airflow leaks from the outer vortex to the inner vortex along the travel path in the cone because the air stream is squeezed.
- The air leak follows a linear model from the top of the cone to the intersection of the vortex interface and the cone walls. At the top of the cone, the airflow rate in the outer vortex is equal to the total inlet airflow rate. At the intersection area, all the air has leaked to the inner vortex and the airflow rate is equal to zero. At any other cross-section between the top and the intersection (in the Z_{o2} range), the outer vortex airflow rate can be quantified using equation 9:

$$Q_z = Q_{in} * \frac{Z}{Z_{o2}} \quad (9)$$

where

Q_z = airflow rate at Z cross-section (at time t)

Q_{in} = inlet airflow rate $\left(Q_{in} = V_{in} * \frac{D_c^2}{8} \right)$

Z = axial component of air stream travel distance at time t

Z_{o2} = axial length of total travel distance in the cone:

$Z_{o2} = 2D_c$ (for 1D3D)

$Z_{o2} = 1.33D_c$ (for 2D2D)

$Z_{o2} = 1.5D_c$ (for 1D2D).

Based on the assumptions described above, the three velocity components in the cone can be determined using equations 10, 11, and 12:

$$V_{t2} = \frac{C}{r} = \frac{R * V_{in}}{r} = \frac{R * V_{in}}{r_o + Z * tg\theta} \quad (10)$$

where

V_{t2} = tangential velocity at time t in the cone
 V_{in} = inlet velocity

R = radius of the barrel ($R = D_c/2$)

r_o = inner vortex and outer vortex interface radius ($r_o = D_e/2$)

Z = axial component of travel distance at time t

θ = cyclone cone angle

$tg\theta = \frac{1}{8}$ (for 1D3D), $tg\theta = \frac{3}{16}$ (for 2D2D),

$tg\theta = \frac{1}{8}$ (for 1D2D).

Then:

$$V_{t2} = \frac{4D_c * V_{in}}{Z + 2D_c} \quad (\text{for 1D3D})$$

$$V_{t2} = \frac{8D_c * V_{in}}{3Z + 4D_c} \quad (\text{for 2D2D})$$

$$V_{t2} = \frac{8D_c * V_{in}}{2Z + 5D_c} \quad (\text{for 1D2D})$$

$$V_{z2} = -\frac{Q_z}{A_z} = \frac{-Q_{in}}{\pi * (R - r_o)} * \frac{1}{\frac{R - r_o}{Z_{o2}} * Z + 2r_o} \quad (11)$$

where

V_{z2} = axial velocity at time t in the cone

Q_z = airflow rate at Z cross-section (at time t)

A_z = outer vortex cross-section area at Z (annular area)

Q_{in} = inlet airflow rate

R = radius of the barrel ($R = D_c/2$)

r_o = inner vortex and outer vortex interface radius ($r_o = D_e/2$)

Z = axial component of travel distance at time t .

Then:

$$V_{z2} = -\frac{4D_c * V_{in}}{(Z + 4D_c) * \pi} \quad (\text{for 1D3D})$$

$$V_{z2} = -\frac{8D_c * V_{in}}{(3Z + 8D_c) * \pi} \quad (\text{for 2D2D})$$

$$V_{z2} = -\frac{16D_c * V_{in}}{(3Z + 15D_c) * \pi} \quad (\text{for 1D2D})$$

$$V_r = V_{z2} * tg\theta \quad (12)$$

The total average velocity and travel distance in the cone can be obtained using the following equations:

$$V_2 = \sqrt{V_{t2}^2 + V_{z2}^2 + V_r^2} \quad (13)$$

$$L_2 = \int_0^{t_2} V_2 dt = \int_{z_{o2}}^0 V_2 * \frac{dz}{V_{z2}} \quad (14)$$

where

L_2 = travel distance in the cone

V_2 = total average velocity in the cone at time t

Z_{o2} = axial length of travel distance in the cone

dz = axial component of travel distance during time dt .

Mathcad (v. 11, Mathsoft Engineering and Education, Inc., Cambridge, Mass.) was used to solve equation 14, and then:

$$L_2 = 10.83D_c \text{ (Mathcad solution for 1D3D)}$$

$$L_2 = 7.22D_c \text{ (Mathcad solution for 2D2D)}$$

$$L_2 = 2.565D_c \text{ (Mathcad solution for 1D2D)}$$

The numbers of turns in the cone can approximately estimated using equation 15:

$$N_2 = \frac{L_2}{\pi * \left(\frac{D_c + D_o}{2} \right)} \quad (15)$$

where

N_2 = number of turns in the cone

L_2 = travel distance in the cone

D_c = cyclone diameter

D_o = inner vortex and outer vortex interface diameter

$$(D_o = D_e).$$

Then:

$$N_2 = 4.60 \text{ (for 1D3D)}$$

$$N_2 = 3.07 \text{ (for 2D2D)}$$

$$N_2 = 1.01 \text{ (for 1D2D)}$$

TOTAL TRAVEL DISTANCE (L) AND NUMBER OF TURNS (N)

As a result of the above calculations, the total travel distance and number of turns for 1D3D, 2D2D, and 1D2D cyclones are listed in the table 3.

Comparison of Number of Turns

Experimentally measured number of turns (Mihalski and Kaspar, 1992), the number of turns calculated using the CCD method (eq. 1), and the number of turns derived from equations (d_{100} or d_{50}) listed in table 1 and research results by Wang et al. (2002) are summarized in table 4 for comparison. The measured number of turns for a traditional 1D3D cyclone (1D3D_t) and a 1D3D cyclone with 2D2D inlet indicate that the number of turns is independent of the inlet height. The CCD model failed to accurately predict the number of turns for a cyclone with an inlet design different from 2D2D (Lapple cyclone; Shepherd and Lapple, 1939). The number of turns derived from d_{100} or d_{50} models listed in table 1 does not agree with experimental measurement for all three cyclone designs.

ANALYSIS OF CYCLONE PRESSURE DROP

In general, cyclone pressure loss can be obtained by summing all individual pressure loss components. The

Table 3. Air stream travel distance and number of effective turns from this study.^[a]

Cyclone Design ^[b]	Barrel		Cone		Total	
	L_1	N_1	L_2	N_2	L	N
1D3D _t	4.8D _c	1.53	10.83D _c	4.60	15.63D _c	6.13
1D3D	4.8D _c	1.53	10.83D _c	4.60	15.63D _c	6.13
2D2D	9.6D _c	3.06	7.22D _c	3.07	16.82D _c	6.13
1D2D	5.2D _c	1.26	2.57D _c	1.01	7.77D _c	2.27

[a] L_1 = travel distance in the barrel part of a cyclone.
 N_1 = number of turns in the barrel part of a cyclone.
 L_2 = travel distance in the cone part of a cyclone.
 N_2 = number of turns in the cone part of a cyclone.
L = total travel distance in a cyclone.
N = number of turns in a cyclone calculated by this study.
[b] 1D3D_t is the traditional 1D3D cyclone shown in figure 2.

Table 4. Comparison of number of turns (N) predicted by different models and experimentally measured.

Cyclone Design ^[a]	Exp. N ^[b]	CCD N ^[c]	Shepherd and Lapple			
			Rosin et al. (1932) N ^[d]	(1940) N ^[e]	(1951) N ^[f]	This Study N
1D3D _t	6.00	2.5	0.37	0.97	0.81	6.13
1D3D	6.00	5.0	0.73	0.97	1.62	6.13
2D2D	5.25	6.0	0.69	0.92	1.61	6.13
1D2D	NA ^[g]	4.0	0.51	0.84	1.92	2.27

[a] 1D3D_t is the traditional 1D3D cyclone shown in figure 2.
[b] The number of turns experimentally measured by Mihalski and Kaspar (1992).
[c] The number of turns in a cyclone calculated by the CCD method (Lapple model, eq. 1).
[d] The number of turns derived from the Rosin et al. (1932) equation (d_{100}) and research results by Wang et al. (2002): $d_{100} = 7.75 \mu\text{m}$ for 1D3D, $d_{100} = 8.25 \mu\text{m}$ for 2D2D, and $d_{100} = 10.75 \mu\text{m}$ for 1D2D (see table 1).
[e] The number of turns derived from the Shepherd and Lapple (1940) equation (d_{100}) and research results by Wang et al. (2002): $d_{100} = 7.75 \mu\text{m}$ for 1D3D, $d_{100} = 8.25 \mu\text{m}$ for 2D2D, and $d_{100} = 10.75 \mu\text{m}$ for 1D2D (see table 1).
[f] The number of turns derived from the Lapple (1951) equation (d_{50}) and research results by Wang et al. (2002): $d_{50} = 4.25 \mu\text{m}$ for 1D3D, $d_{50} = 4.40 \mu\text{m}$ for 2D2D, and $d_{50} = 4.50 \mu\text{m}$ for 1D2D (see table 1).
[g] NA = data not available.

following pressure loss components are involved in the analysis of cyclone pressure loss for this research:

- Cyclone entry loss (ΔP_e).
- Kinetic energy loss (ΔP_k).
- Frictional loss in the outer vortex (ΔP_f).
- Kinetic energy loss caused by the rotational field (ΔP_r).
- Pressure loss in the inner vortex and exit tube (ΔP_o).

Cyclone Entry Loss (ΔP_e)

Cyclone entry loss is the dynamic pressure loss in the inlet duct and can be determined by:

$$\Delta P_e = C_2 * VP_{in} \quad (16)$$

where

ΔP_e = cyclone entry loss (dynamic pressure loss in the inlet duct)

C_2 = dynamic loss constant ($C_2 \approx 1$)

VP_i = inlet velocity pressure.

Kinetic Energy Loss (ΔP_k)

Kinetic energy loss is caused by the area change (velocity change) from the inlet tube to the outlet tube. It can be calculated by:

$$\Delta P_k = VP_{in} - VP_{out} \quad (17)$$

where

ΔP_k = kinetic energy loss

VP_i = inlet velocity pressure

VP_o = outlet velocity pressure.

Frictional Loss in the Outer Vortex (ΔP_f)

The frictional pressure loss is the pressure loss in the cyclone outer vortex caused by the friction of the wall surface. In the outer vortex, the air stream flows in a downward spiral through the cyclone. It may be considered that the air stream travels in an imaginary spiral tube with diameter D_s and length L (the air stream travel distance in the

outer vortex, fig. 5). The frictional pressure loss can be determined by Darcy's equation:

$$d\Delta P_f = f * \frac{VP_s}{D_s} * dL \quad (18)$$

where

- $d\Delta P_f$ = frictional pressure loss at travel distance dL
- f = friction factor, dimensionless
- dL = air stream travel distance in the outer vortex during time dt
- D_s = equivalent stream diameter at time t
- VP_s = stream velocity pressure at time t .

Frictional Loss in the Barrel (ΔP_{f1}): The equivalent stream diameter (D_{s1}) was used to quantify the size of the oval-shaped stream (the stream in the imaginary spiral tube). The flow rate and total velocity of the stream determine this equivalent diameter, as shown in equation 19:

$$V_{s1} * \frac{\pi * D_{s1}^2}{4} = V_{in} * \frac{D_c^2}{8} \quad (19)$$

where

- V_{s1} = air stream velocity in the barrel part ($V_{s1} = V_1$ determined by eq. 6)
- D_{s1} = equivalent stream diameter in the barrel
- D_c = cyclone diameter
- V_{in} = inlet velocity.

Then

$$D_{s1} = 0.395D_c \text{ for 1D3D, 2D2D, and 1D2D.}$$

The friction pressure loss in the barrel part can be determined as follows:

$$\Delta P_{f1} = \int_0^{L_1} f * \frac{VP_{s1}}{D_{s1}} dL = \int_0^{Z_1} f * \frac{VP_{s1}}{D_{s1}} * V_1 * \frac{dz}{V_{z1}} \quad (20)$$

where

- ΔP_{f1} = frictional loss in the barrel
- L_1 = travel distance in the barrel
- f = friction factor
- VP_{s1} = stream velocity pressure at time t in the barrel

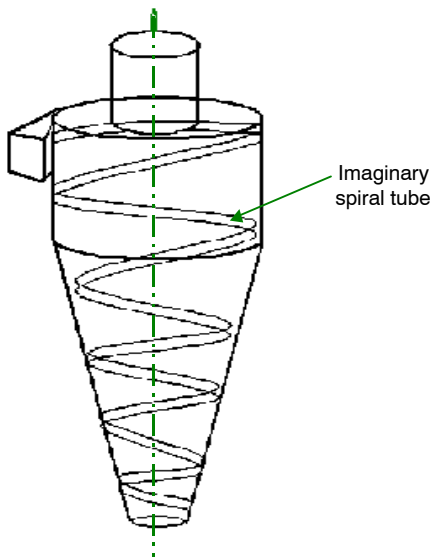


Figure 5. Imaginary spiral tube of air stream in the outer vortex.

- D_{s1} = stream diameter at time t in the barrel
- dL = air stream travel distance in the outer vortex at time dt
- V_1 = air stream total velocity at time t in the barrel
- V_{z1} = axial velocity component in the barrel at time t
- Z_1 = length of the barrel
- dz = axial component of travel distance during the time dt .

In equation 20, VP_{s1} is the stream velocity pressure determined by stream velocity V_{s1} . The friction factor (f) is a function of the Reynolds number (R_e , eq. 21) and the degree of roughness of the imaginary spiral tube surface:

$$R_e = \frac{D * V * \rho}{\mu} \quad (21)$$

The friction factor (f) can be obtained from the Moody chart (the friction chart) based upon the relative roughness factor (e/D) of the tube surface and the fluid Reynolds number. In this case, since the imaginary tube consists of the cyclone inside surface on one side and the air stream on the other side, one-half of the friction factors obtained from the chart were used for pressure drop calculation in equation 20. Table 5 lists some of the friction factors for 1D3D, 2D2D, and 1D2D cyclones at their respective design inlet velocities.

Equation 20 is the friction loss model for the barrel part of a cyclone. This model indicates that the friction pressure loss is a function of the air stream travel distance in the outer vortex of the barrel. In other words, the friction loss is a function of the cyclone height: the higher the cyclone body, the higher the friction loss. The following results were obtained from equation 20 for predicting friction loss in the barrel part of a cyclone:

$$\Delta P_{f1} = 0.13 * VP_{s1} = 0.14 * VP_{in} \quad (\text{for 1D3D})$$

$$\Delta P_{f1} = 0.27 * VP_{s1} = 0.28 * VP_{in} \quad (\text{for 2D2D})$$

$$\Delta P_{f1} = 0.14 * VP_{s1} = 0.15 * VP_{in} \quad (\text{for 1D2D}) \quad (22)$$

Frictional Loss in the Cone (ΔP_{f2}): In the cone part of a cyclone, the equivalent stream diameter (D_{s2}) is determined by:

$$V_{s2} * \frac{\pi * D_{s2}^2}{4} = V_{in} * \frac{D_c^2}{8} * \frac{Z}{Z_{o2}} \quad (23)$$

where

- V_{s2} = air stream velocity in the cone ($V_{s2} = V_2$ determined by eq. 13)
- D_{s2} = equivalent stream diameter in the cone
- D_c = cyclone diameter
- V_{in} = inlet velocity

Table 5. Friction factors (f) for friction pressure loss calculation.

Cyclone Design	Size (D_c)	e/D_c	Reynolds Number	f	
				Moody Chart	For ΔP_f Models
1D3D	0.2 m (6 in.)	0.0010	1.64×10^5	0.022	0.011
	0.9 m (36 in.)	0.0002	9.85×10^5	0.016	0.008
2D2D	0.2 m (6 in.)	0.0010	1.54×10^5	0.022	0.011
	0.9 m (36 in.)	0.0002	9.20×10^5	0.015	0.008
1D2D	0.2 m (6 in.)	0.0010	1.23×10^5	0.023	0.012
	0.9 m (36 in.)	0.0002	7.40×10^5	0.015	0.008

Z = axial component of air stream travel distance at time t in the cone

Z_{o2} = axial length of total travel distance in the cone.

The friction pressure loss in the cone can be determined as follows:

$$\Delta P_{f2} = \int_0^{L_2} f * \frac{VP_{s2}}{D_{s2}} dL = \int_{Z_{o2}}^0 f * \frac{VP_{s2}}{D_{s2}} * V_2 * \frac{dz}{V_{z2}} \quad (24)$$

where

ΔP_{f2} = frictional loss in the cone

L_2 = travel distance in the cone

f = friction factor

VP_{s2} = stream velocity pressure at time t in the cone

D_{s2} = stream diameter at time t in the cone

dL = air stream travel distance in the outer vortex at time dt

V_2 = air stream total velocity at time t in the cone

V_{z2} = axial velocity component in the cone

Z_{o2} = axial component of travel distance in cone

dz = axial component of travel distance during the time dt .

The solutions of equation 24 are the models used to predict friction loss in the cone part of a cyclone. The friction factor (f) is given in table 5. Again, the above models indicate that the friction loss in the cone is a function of air stream travel distance in the outer vortex of the cone. Therefore, the friction loss in the cone is a function of the height of the cone.

Kinetic Energy Loss Caused by the Rotational Field (ΔP_r)

In the cyclone cone, the rotation of the airflow establishes a pressure field because of radial acceleration. The rotational energy loss is the energy that is used to overcome centrifugal force and allow the air stream to move from the outer vortex to the inner vortex. To develop an equation for the rotational kinetic energy loss, it is assumed that the direction of rotation is the same in both the inner and outer vortex so that little friction is to be expected at their interface (the junction point).

The rotational loss can be quantified as the pressure change in the pressure field from the cone wall to the vortex interface:

$$dP = \rho * \frac{V_t^2}{r} * dr \quad (25)$$

where

dP = pressure gradient from outer vortex to inner vortex at radius r

ρ = air density

r = radius

V_t = tangential velocity at radius r .

Solving equation 25, the rotational loss can be obtained as the follows:

$$\Delta P_r = \rho * V_{in}^2 * \left(\frac{R}{r_o} - 1 \right) \quad (26)$$

Then:

$\Delta P_r = 2 VP_{in}$ (for 1D3D and 2D2D)

$\Delta P_r = 1.22 VP_{in}$ (for 1D2D)

where

ΔP_r = rotational pressure loss

ρ = air density

V_{in} = inlet velocity

R = cyclone radius

r_o = radius of the vortex interface

VP_{in} = inlet velocity pressure.

Pressure Loss in the Inner Vortex and Exit Tube (ΔP_o)

The inner vortex is assumed to have a constant height of spiral, a constant angle of inclination to the horizontal, and the same rotational velocity at the same radius at any vertical position. The method of calculation for this part of the pressure component will be to determine the average pressure loss in the inner vortex and the exit tube. This can be determined as follows:

$$\Delta P_o = C_3 * VP_{out} \quad (27)$$

where

ΔP_o = pressure loss in the inner vortex and exit tube

C_3 = dynamic loss constant ($C_3 \approx 1.8$)

VP_{out} = outlet velocity pressure.

Cyclone Total Pressure Loss (ΔP_{total})

The total pressure loss in the cyclone is obtained by simply summing up the five pressure drop components as follows:

$$\Delta P_{total} = \Delta P_e + \Delta P_k + \Delta P_f + \Delta P_r + \Delta P_o \quad (28)$$

CYCLONE PRESSURE DROP PREDICTIONS

Equations 16, 17, 22, 24, 26, and 27 are the models used to predict five pressure loss components. Based on these models, pressure drops for different sizes of cyclones with different inlet velocities were calculated. Predicted pressure drops for 1D3D, 2D2D, and 1D2D cyclones with their respective design velocities are listed in table 6. Pressure drops predicted using the CCD method are also included in table 6 for comparison. The predictions of pressure drop in table 6 indicate: (1) cyclone pressure drop is independent of cyclone size; (2) frictional loss in the outer vortex and rotational energy loss in a cyclone are the major pressure loss components; (3) frictional loss is a function of cyclone height (the higher a cyclone, the higher the friction loss); and (4) predictions of pressure drop using the CCD method tend to be higher than the predictions from this research.

TESTING OF THE NEW METHOD

SYSTEM SETUP

An experiment was conducted to measure cyclone pressure drops at different inlet velocities for the comparison of measured pressure drop versus pressure drop predicted by the new theory developed in this research. The experimental setup is shown in figure 6. The tested cyclones were 0.2 m (6 in.) in diameter. Pressure transducers (model PX274, output = 4 to 20 mA, accuracy = $\pm 1.0\%$ of full scale, Omega Engineering, Stamford, Conn.) and data loggers (HOB0 H8 RH/Temp/2x External, range = 0 to 20 mA, accuracy = $\pm 1.0\%$ of full scale, Onset Computer Corp., Bourne, Mass.) were used to obtain the differential pressure from the cyclone inlet and outlet and the pressure drop across the orifice meter.

The orifice pressure drop was used to monitor the system airflow rate by the following relationship:

Table 6. Predicted pressure drops for 1D3D, 2D2D, and 1D2D cyclones.

Cyclone ^[a] Size	ΔP_e ^[b]	ΔP_k ^[c]	ΔP_f ^[d]		ΔP_r ^[e]	ΔP_o ^[f]	Total ΔP ^[g]	CCD ΔP ^[h]
			ΔP_{f1}	ΔP_{f2}				
1D3D at $V_{in} = 16$ m/s (3200 ft/min) ^[i]								
0.1 (4)	159 (0.64)	95 (0.38)	22 (0.09)	359 (1.44)	319 (1.28)	117 (0.47)	1071 (4.30)	1189 (4.77)
0.3 (12)	159 (0.64)	95 (0.38)	22 (0.09)	359 (1.44)	319 (1.28)	117 (0.47)	1071 (4.30)	1189 (4.77)
0.9 (36)	159 (0.64)	95 (0.38)	22 (0.09)	359 (1.44)	319 (1.28)	117 (0.47)	1071 (4.30)	1189 (4.77)
2D2D at $V_{in} = 15$ m/s (3000 ft/min)								
0.1 (4)	140 (0.56)	82 (0.33)	40 (0.16)	212 (0.85)	279 (1.12)	103 (0.41)	854 (3.43)	1045 (4.20)
0.3 (12)	140 (0.56)	82 (0.33)	40 (0.16)	212 (0.85)	279 (1.12)	103 (0.41)	854 (3.43)	1045 (4.20)
0.9 (36)	140 (0.56)	82 (0.33)	40 (0.16)	212 (0.85)	279 (1.12)	103 (0.41)	854 (3.43)	1045 (4.20)
1D2D at $V_{in} = 12$ m/s (2400 ft/min)								
0.1 (4)	89 (0.36)	75 (0.30)	12 (0.05)	80 (0.32)	107 (0.43)	27 (0.11)	392 (1.57)	428 (1.72)
0.3 (12)	89 (0.36)	75 (0.30)	12 (0.05)	80 (0.32)	107 (0.43)	27 (0.11)	392 (1.57)	428 (1.72)
0.9 (36)	89 (0.36)	75 (0.30)	12 (0.05)	80 (0.32)	107 (0.43)	27 (0.11)	392 (1.57)	428 (1.72)

- [a] Cyclone size in m (in.).
- [b] ΔP_e = cyclone entry pressure drop in Pa (inch H₂O).
- [c] ΔP_k = kinetic energy loss in Pa (inch H₂O).
- [d] ΔP_f = frictional loss in the outer vortex in Pa (inch H₂O): ΔP_{f1} = frictional loss in the barrel, and ΔP_{f2} = frictional loss in the cone.
- [e] ΔP_r = kinetic loss caused by the rotational field in Pa (inch H₂O).
- [f] ΔP_o = pressure loss in the inner vortex and exit tube in Pa (inch H₂O).
- [g] Total ΔP = cyclone pressure drop predicted by this research in Pa (inch H₂O).
- [h] CCD ΔP = cyclone pressure drop predicted using the CCD method (eqs. 2 and 3, using $K = 15$ and $\rho_g = 1.2$ kg/m³) in Pa (inch H₂O).
- [i] V_{in} = cyclone inlet velocity in m/s (ft/min).

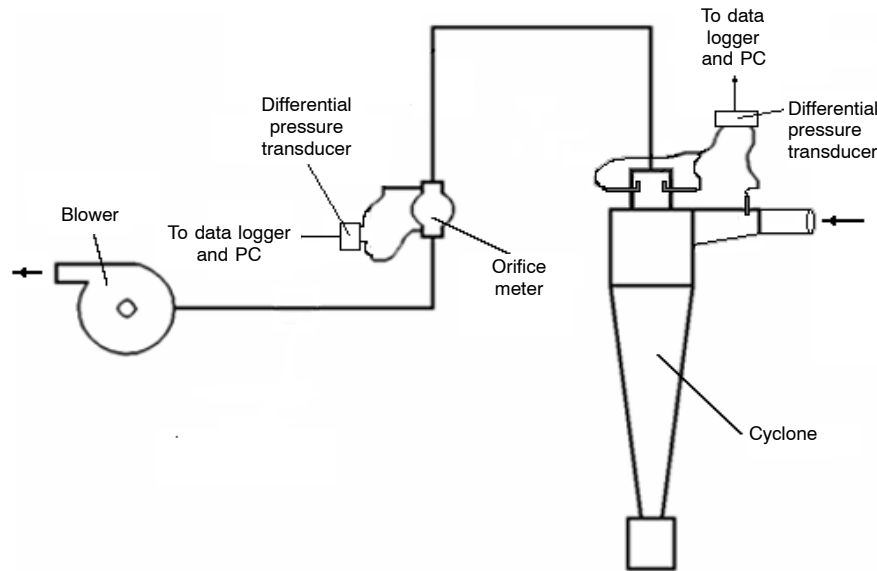


Figure 6. Pressure drop measurement system setup.

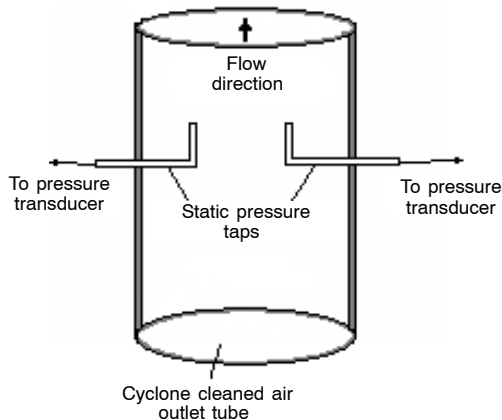


Figure 7. Static pressure taps in a cyclone outlet tube for pressure drop measurement.

$$Q = 3.478 * K * D_o^2 * \sqrt{\frac{\Delta P}{\rho_a}} \quad (29)$$

where

Q = airflow rate through the orifice meter (m³/s)

K = flow coefficient (dimensionless)

D_o = orifice diameter (m)

ΔP = pressure drop cross the orifice (mm H₂O)

ρ_a = air density (kg/m³).

A problem was observed during the tests. In the outlet tube, the air stream spirals upward. This spiral path caused some difficulties in measuring static pressure in the outlet tube. In order to measure the static pressure drop through the cyclone, three evenly distributed static pressure taps (fig. 7) were made and inserted into the air stream in such a way that

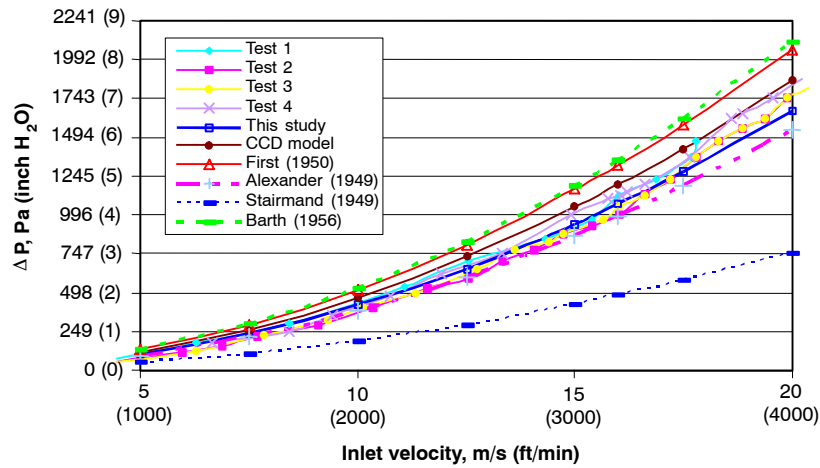


Figure 8. Measured and calculated pressure drops vs. inlet velocities for 1D3D cyclone.

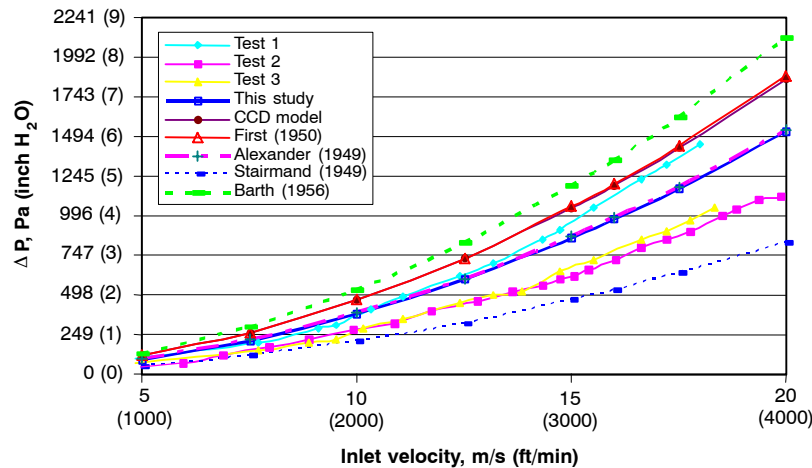


Figure 9. Measured and calculated pressure drops vs. inlet velocities for 2D2D cyclone.

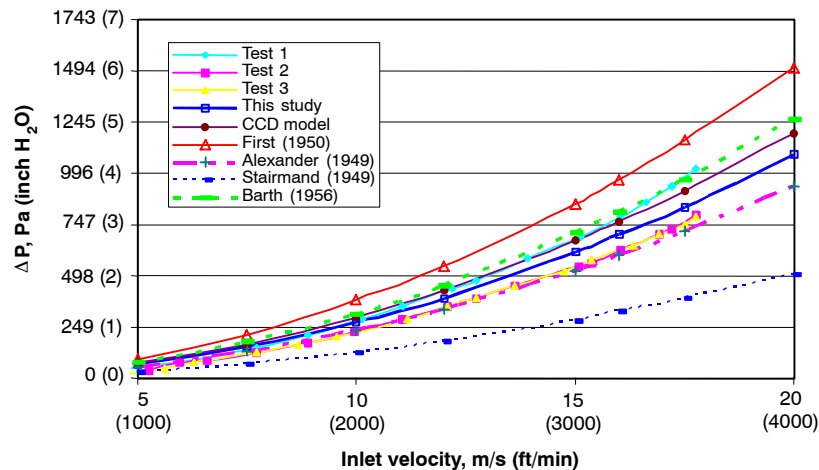


Figure 10. Measured and calculated pressure drops vs. inlet velocities for 1D2D cyclone.

the static pressure sensing position was in the direction of the airflow to avoid velocity pressure. It is desirable to keep one side of the static pressure tap perpendicular to the wall of the cyclone outlet tube and the other side of the static pressure tap parallel to the flow direction (fig. 7). If the static pressure taps were not placed properly in the exit tube, the measurement would include part of velocity pressure, instead of static pressure only.

COMPARISONS OF THEORETICAL PREDICTIONS WITH TESTING RESULTS

Three tests were performed on 2D2D and 1D2D cyclone designs and four tests were performed on a 1D3D cyclone design at different inlet velocities. For the 1D3D cyclone, tests 1, 2, and 3 were conducted on a 0.2 m (6 in.) cyclone and test 4 was on a 0.1 m (4 in.) cyclone.

Table 7. Experimental and predicted cyclone pressure drops in Pa (inch H₂O) at design inlet velocity.^[a]

Cyclone Design	Experimental ΔP ^[b]	This Study ΔP	CCD ΔP	First (1950) ΔP	Alexander (1949) ΔP	Stairmand (1949) ΔP	Barth (1956) ΔP
1D3D	1053 (4.23)	1071 (4.30)	1188 (4.77)	1320 (5.30)	984 (3.95)	481 (1.93)	1350 (5.42)
2D2D	760 (3.05)	854 (3.43)	1046 (4.20)	1053 (4.23)	864 (3.47)	466 (1.87)	1185 (4.76)
1D2D	374 (1.51)	392 (1.57)	429 (1.72)	543 (2.18)	336 (1.35)	182 (0.73)	453 (1.82)

^[a] Inlet design velocity: $V_{1D3D} = 16$ m/s, $V_{2D2D} = 15$ m/s, and $V_{1D2D} = 12$ m/s.

^[b] Average ΔP from tests 1, 2, and 3.

Figures 8 through 10 show the comparison of the predicted and measured cyclone pressure drop curves (pressure drops vs. inlet velocity). For the 1D3D cyclone, there were no significant pressure drop differences among tests 1, 2, 3, and 4 (fig. 8). As mentioned before, tests 1, 2, and 3 were conducted on a 0.2 m (6 in.) cyclone and test 4 was conducted on a 0.1 m (4 in.) cyclone. Therefore, the measured results indicate that pressure drop is independent of cyclone size.

For the 2D2D and 1D2D cyclones (figs. 9 and 10), the results of test 1 are significantly different from the results of tests 2 and 3. This was caused by not placing the static pressure taps in a good position. Three evenly distributed (around the wall of outlet tube) static pressure taps were initially placed in position such that one end of each tap was in the direction of airflow (fig. 7). These taps were glued to the wall of outlet tube. However, it was observed that the positions of the static pressure taps were deflected due to the glue not being completely dry. This caused the taps to be not totally in the direction of the flow, and some velocity pressure was added. As a result, the results of test 1 are significantly higher than the results of tests 2 and 3. The taps were re-positioned to the correct direction after test 1.

Pressure drop curves using CCD and the four other models listed in the table 2 are also included in figures 8 through 10. Comparisons of the pressure drop curves predicted by the different models and the experimental measurements indicate that the CCD, First, and Barth models tended to predict higher pressure drops for all three cyclone designs, whereas the Stairmand model tended to predict lower pressure drops for all three cyclone designs. Among all the models, this study and the Alexander model tended to give better predictions of pressure drops for all three cyclone designs.

For the 2D2D cyclone design, there is a significant difference between the pressure drops predicted by this study and the test results. This could have been caused by inaccurate measurements due to introducing some velocity pressure into the measurements through deflection of the static pressure taps, as mentioned before.

Table 7 lists comparisons of the pressure drops predicted by the different models for 1D3D, 2D2D, and 1D2D cyclones at their own design inlet velocity, i.e., 16 m/s (3200 fpm), 15 m/s (3000 fpm), and 12 m/s (2400 fpm), respectively. The comparisons illustrate that this study gave pressure drop predictions that were closest to the experimental data. The pressure drops predicted by this study are 1071, 854, and 392 Pa (4.3, 3.43, and 1.57 inch H₂O) for the 1D3D, 2D2D, and 1D2D cyclone designs, respectively. Results in table 7 also verify that the theoretical predictions of pressure drop obtained by this study are in excellent agreement with experimental measurements. Thus, the new theoretical methods developed in this research for predicting cyclone pressure drop are reliable.

CONCLUSIONS

Air stream travel distance and effective number of turns can be determined based on the velocity profile in a cyclone. Theoretical analysis shows that the number of turns is determined by the cyclone design and is independent of cyclone diameter and inlet velocity. This study predicted 6.13 turns in 1D3D and 2D2D cyclones and 2.27 turns in a 1D2D cyclone. Cyclone pressure drop consists of five individual pressure drop components. The frictional loss in the outer vortex and the rotational energy loss in the cyclone are the major pressure loss components. The theoretical analyses of the pressure drop for different size cyclones (4, 12, and 36 in.) showed that cyclone pressure drop is independent of cyclone diameter. Experiments were conducted to verify the theoretical analysis results obtained by this study, the CCD method, and several other theoretical models in the literature. Comparisons of pressure drops predicted by different theoretical models and the experimental measurements verified that this study gave pressure drop predictions that were closest to the experimental data, and the theoretical predictions of pressure drop obtained by this study are in excellent agreement with experimental measurements. The new theoretical method can be used to predict the air stream travel distance, number of turns, and cyclone pressure drop.

REFERENCES

- Alexander, R. M. 1949. Fundamentals of cyclone design and operation. In *Proc. Australasian Inst. Min. Met.* (New Series) 152-3: 203-228.
- Barth, W. 1956. Design and layout of the cyclone separator on the basis of new investigations. *Brenn. Warme Kraft* 8: 1-9.
- Cooper, C. C., and G. C. Alley. 2002. *Air Pollution Control: A Design Approach*. Prospect Heights, Ill.: Waveland Press.
- Davis, W. T. 2000. *Air Pollution Engineering Manual*. 2nd ed. Air and Waste Management Association. New York, N.Y.: John Wiley and Sons.
- Doerschlag, C., and G. Miczek. 1977. Cyclone dust collector. *Chemical Eng.* 84(4): 64-72.
- Fayed, M. E., and L. Otten. 1997. *Handbook of Powder Science and Technology*. 2nd ed. New York, N.Y.: Chapman and Hall.
- First, M. W. 1950. Fundamental factors in the design of cyclone dust collectors. PhD diss. Cambridge, Mass.: Harvard University.
- Funk, P. A., R. W. Clifford, and S. E. Hughs. 1999. Optimum entry velocity for modified 1D3D cyclones. ASAE Paper No. 994198. St. Joseph, Mich.: ASAE.
- Holt, G., and R. V. Baker. 1999. Evaluation of PM₁₀ and TSP emissions from modified 1D3D cyclones. ASAE Paper No. 991130. St. Joseph, Mich.: ASAE.
- Lapple, C. E. 1951. Processes use many collector types. *Chemical Eng.* 58(5): 144-151.
- Leith, D., and D. Mehta. 1973. Cyclone performance and design. *Atmospheric Environ.* 7: 527-549.

- Mihalski, K., and P. Kaspar. 1992. Optimum utilization of cyclone technology. ASAE Paper No. 921040. St. Joseph, Mich.: ASAE.
- Mihalski, K., P. Kaspar, and C. B. Parnell, Jr. 1993. Design of pre-separators for cyclone collectors. In *Proc. 1993 Beltwide Cotton Production Conferences*, 1561-1568. Memphis, Tenn.: National Cotton Council.
- Parnell, C. B. Jr., and D. D. Davis. 1979. Predicted effects of the use of new cyclone designs on agricultural processing particle emissions. ASAE Paper No. SWR-79040. St. Joseph, Mich.: ASAE.
- Rosin, P., E. Rammler, and E. Intelmann. 1932. *V.D.I. (Ver. Deut. Ing.) Z.* 76: 433.
- Simpson, S., and C. B. Parnell, Jr. 1995. New low-pressure cyclone design for cotton gins. In *Proc. 1995 Beltwide Cotton Production Conferences*, 680-687. Memphis, Tenn.: National Cotton Council.
- Shepherd, C. B., and C. E. Lapple. 1939. Flow pattern and pressure drop in cyclone dust collectors. *Industrial and Eng. Chemistry* 31(8): 972-984.
- Shepherd, C. B., and C. E. Lapple. 1940. Flow pattern and pressure drop in cyclone dust collectors. *Industrial and Eng. Chemistry* 32: 1246-1248.
- Stairmand, C. J. 1949. Pressure drop in cyclone separators. *Industrial and Eng. Chemistry* 16(B): 409-411.
- Stairmand, C. J. 1951. The design and performance of cyclone separators. *Trans. Chemical Eng.* 29(1): 356-373.
- Stern, A. C., K. J. Caplan, and P. D. Bush. 1955. Cyclone dust collectors. API report. Washington, D.C.: American Petroleum Institute.
- Ter Linden, A. J. 1949. Investigation into cyclone dust collectors. *Ins. Mech. Engrs.* 160: 233-240.
- Wang, L. 2000. A new engineering approach to cyclone design for cotton gins. MS thesis. College Station, Texas: Texas A&M University, Department of Agricultural Engineering.
- Wang, L., C. B. Parnell, and B. W. Shaw. 1999. Performance characteristics for the 1D2D, 2D2D, 1D3D, and barrel cyclones. ASAE Paper No. 994195. St. Joseph, Mich.: ASAE.
- Wang, L., C. B. Parnell, and B. W. Shaw. 2002. Study of the cyclone fractional efficiency curves. *Agric. Eng. Intl.* Vol. IV: Manuscript BC 02 002. Available at: <http://cigr-ejournal.tamu.edu>.

